



## Hit-to-lead investigation of a series of novel combined dopamine D<sub>2</sub> and muscarinic M<sub>1</sub> receptor ligands with putative antipsychotic and pro-cognitive potential

Anette Graven Sams<sup>a,\*</sup>, Krestian Larsen<sup>a</sup>, Gitte Kobberø Mikkelsen<sup>a</sup>, Morten Hentzer<sup>a</sup>, Claus Tornby Christoffersen<sup>a</sup>, Klaus Gjervig Jensen<sup>b</sup>, Kristen Frederiksen<sup>a</sup>, Benny Bang-Andersen<sup>a</sup>

<sup>a</sup> Neuroscience Drug Discovery Denmark, H. Lundbeck A/S, 9 Ottolievej, DK-2500 Copenhagen-Valby, Denmark

<sup>b</sup> Drug ADME Research, H. Lundbeck A/S, 9 Ottolievej, DK-2500 Copenhagen-Valby, Denmark

### ARTICLE INFO

#### Article history:

Received 26 March 2012

Revised 9 May 2012

Accepted 10 May 2012

Available online 18 May 2012

#### Keywords:

Schizophrenia

Cognition

D<sub>2</sub>

M<sub>1</sub>

### ABSTRACT

We describe the discovery of a series of compounds based on 1-{3-[4-(2-oxo-2,3-dihydro-benzimidazol-1-yl)-piperidin-1-yl]-propyl}-3,4-dihydro-1*H*-quinolin-2-one (**3**), showing combined D<sub>2</sub> receptor affinity and M<sub>1</sub> receptor agonism. Based on a strategy of controlling log*P*, we herein describe a hit-to-lead investigation with the aim of retaining the combined D<sub>2</sub>/M<sub>1</sub> profile, while removing the propensity of the compounds to inhibit the hERG channel, as well as at obtaining acceptable pharmacokinetic properties. Although a SAR was evident for all four parameters in question, it was not possible to separate hERG channel inhibition and D<sub>2</sub> receptor affinity by this effort; whilst it was feasible to obtain compounds with M<sub>1</sub> receptor agonism, acceptable clearance, and weak hERG inhibition.

© 2012 Elsevier Ltd. All rights reserved.

Schizophrenia is a debilitating psychiatric disorder, which is characterized by the presence of three major symptom clusters. These include positive symptoms, such as delusions, hallucinations and disordered speech; negative symptoms, including social withdrawal and anhedonia; and cognitive symptoms. The cognitive symptoms are evident in patients even before the onset of the first psychotic episode, and have been suggested to be the core symptoms of the disease.<sup>1</sup> The cognitive impairment affect several cognitive domains, particularly working memory and executive function (the ability to plan and execute tasks).<sup>2</sup> The cognitive impairment associated with schizophrenia (CIAS) negatively impacts the patients' quality of life, and are untreated by current antipsychotic drugs.<sup>3</sup> Treatment of CIAS is regarded as a major unmet medical need.

It has been suggested that activation of muscarinic M<sub>1</sub> receptors could play a role in the treatment of CIAS.<sup>4–7</sup> For example, muscarinic M<sub>1</sub> receptor expression is decreased in cortical regions of schizophrenic patients,<sup>8,9</sup> and M<sub>1</sub> receptor knock-out mice revealed deficits in hippocampus and prefrontal cortex dependent working and episodic memory tasks.<sup>10,11</sup>

\* Corresponding author at present address: LEO Pharma A/S, Industriparken 55, 2750 Ballerup, Denmark. Tel.: +45 41772172.

E-mail address: [anette.sams@leo-pharma.com](mailto:anette.sams@leo-pharma.com) (A.G. Sams).

We hypothesised that compounds with a combined pharmacological profile of D<sub>2</sub> receptor antagonism and M<sub>1</sub> receptor agonism could have antipsychotic as well as a pro-cognitive potential.<sup>3</sup> Indeed, the major human metabolite of the antipsychotic drug clozapine, *N*-desmethyl clozapine (NDMC), with a broad pharmacological profile including D<sub>2</sub> receptor antagonism and M<sub>1</sub> receptor agonism, was pursued as a putative antipsychotic with pro-cognitive potential. NDMC was progressed into phase 2 clinical trials, although it failed to show antipsychotic efficacy as mono-therapy.<sup>12,13</sup> Accordingly, we compiled a focused library by a virtual in silico screen of the corporate compound file, using a D<sub>2</sub> receptor pharmacophore model. Approximately 10,000 compounds were selected and subsequently screened in a D<sub>2</sub> receptor binding assay.<sup>14</sup> The same compound collection was screened for functional agonism at the human M<sub>1</sub> receptor.<sup>15</sup> From this screen, compounds **1** and **2**, having the desired combined D<sub>2</sub> and M<sub>1</sub> receptor profile, were identified (Chart 1). Compound **1** (Oxiperomid, R4714) displayed high affinity for the D<sub>2</sub> receptor (*K*<sub>i</sub> = 5.5 nM), for comparison, the antipsychotic drug haloperidol (Chart 1) exerts a similar level of D<sub>2</sub> receptor affinity (*K*<sub>i</sub> = 3.0 nM). Furthermore, it was shown that compound **1** was a partial M<sub>1</sub> receptor agonist with an EC<sub>50</sub> value of 400 nM and *E*<sub>max</sub> = 78%, relative to an *E*<sub>max</sub> of 100% for acetylcholine (ACh). The EC<sub>50</sub> of ACh in the assay is 1.1 nM. For reference, we have recently demonstrated a pro-cognitive effect of the allosteric M<sub>1</sub> receptor agonist Lu AE51090 (**4**), which has an EC<sub>50</sub> value of 61 nM and an *E*<sub>max</sub> = 83% in the same assay.<sup>15</sup> Compared to **1**, hit compound **2**

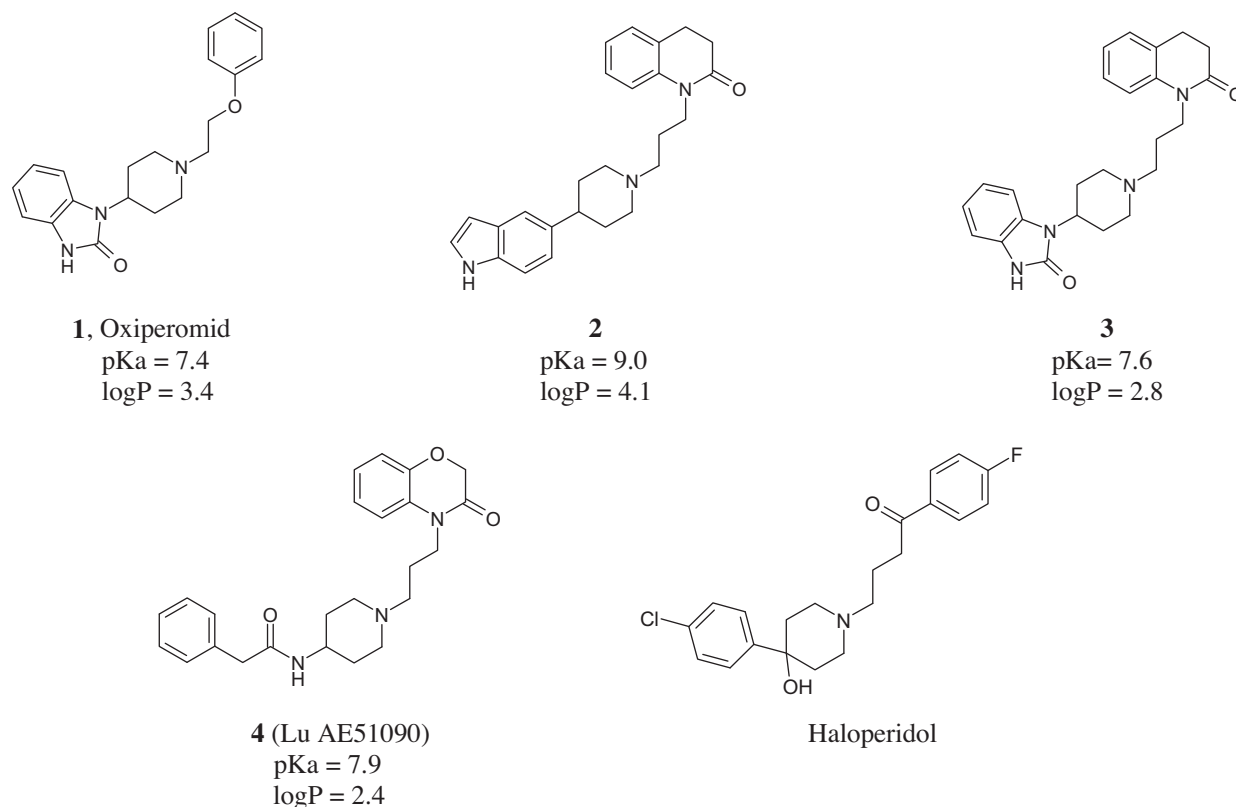


Chart 1.

showed a weaker D<sub>2</sub> receptor affinity ( $K_i$  = 42 nM), but a similar profile at the M<sub>1</sub> receptor, being a partial agonist with an EC<sub>50</sub> value of 160 nM and  $E_{max}$  = 70%.

Incubation of **1** and **2** with human liver microsomes (HLM) suggested that **1** had an acceptable intrinsic hepatic clearance ( $hCl_{int}$  = 1.4 L/min), while **2** showed a high intrinsic hepatic clearance ( $hCl_{int}$  = 9 L/min). For comparison, the human liver–blood flow (LBF) is 1.4 L/min. Compounds **1** and **2** were also tested for inhibition of Rb<sup>+</sup> flux through the hERG channel,<sup>16</sup> and were found to inhibit the channel with IC<sub>50</sub> values of 2.1  $\mu$ M and 4.4  $\mu$ M, respectively.

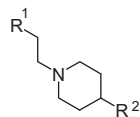
We decided not to invest further in hit compound **2**, mainly due to the suggested poor pharmacokinetic properties. The similarities between **1** and **2** inspired us to design compound **3**, combining structural features from both initial hits. Compound **3** retained the combined D<sub>2</sub>/M<sub>1</sub> receptor profile of its progenitors, displaying a high D<sub>2</sub> receptor affinity ( $K_i$  = 9.5 nM) as well as M<sub>1</sub> receptor partial agonism (EC<sub>50</sub> = 110 nM,  $E_{max}$  = 53%). The intrinsic clearance in HLM incubations was high ( $hCl_{int}$  = 3.9 L/min). High in vivo clearance (3 L/h/kg) was also observed the rat, in good agreement with high intrinsic clearances measured in vitro using rat liver microsome incubations ( $Cl_{int}$  = 130 ml/min, rat LBF=20 ml/min) and rat hepatocyte incubations ( $Cl_{int}$  = 160 ml/min). This suggested that **3**

was mainly cleared by hepatic metabolism in rat. The similar clearance rates obtained from rat microsomes (predominantly phase I enzymes) and hepatocytes (both phase I and phase II enzymes), indicated predominant phase I clearance of **3**. Thus, HLM incubation was used for monitoring clearance during investigation of the series.<sup>17</sup> Furthermore, **3** was found to inhibit the hERG channel with an IC<sub>50</sub> value of 7.3  $\mu$ M. Compound **4**, which is structurally related to **3**, shows comparatively weaker hERG channel inhibition, with an IC<sub>50</sub> value of 20  $\mu$ M, and for a series of analogues of **4**, we have shown that the pharmacokinetic properties can be modulated.<sup>15</sup> These observations indicated to us that hERG inhibition and metabolic stability might be modulated within a series of compounds based on **3**. Compound **3** was further profiled in functional hM<sub>2</sub>–hM<sub>5</sub> assays,<sup>15</sup> and showed no agonism at any of these muscarinic receptor subtypes. This was encouraging, as moderate selectivity for hM<sub>1</sub> receptors over the other muscarinic receptor subtypes, especially hM<sub>2</sub> and hM<sub>3</sub> receptors, has been suggested to cause the peripheral cholinergic side effects observed with orthosteric M<sub>1</sub> receptor agonists in clinical investigations.<sup>5,18,19</sup> The structural similarity of **3** and **4** suggested that **3** was an allosteric hM<sub>1</sub> agonist in analogy with **4**.<sup>15</sup> To investigate this in more detail, compound **3** was assayed for activity at the hM<sub>1</sub> Y381A receptor mutant, in which the essential tyrosine residue 381 located in the transmem-

**Table 1**  
Functional agonism of **3** at muscarinic receptors<sup>a</sup>

Compound	hM <sub>1</sub> Y381A		hM <sub>2</sub>		hM <sub>3</sub>		hM <sub>4</sub>		hM <sub>5</sub>	
	EC <sub>50</sub> (nM)	E <sub>max</sub> (%)	EC <sub>50</sub> (nM)	E <sub>max</sub> (%)	EC <sub>50</sub> (nM)	E <sub>max</sub> %	EC <sub>50</sub> (nM)	E <sub>max</sub> (%)	EC <sub>50</sub> (nM)	E <sub>max</sub> (%)
ACh	27000	100	220	100	3.2	100	10	100	1.2	100
<b>3</b>	6.3	89	n.d.	0%	n.d.	0%	n.d.	8%	n.d.	0%

<sup>a</sup> Data are means of two experiments Activity at 10  $\mu$ M test concentration tested is given when an EC<sub>50</sub> could not be established. n.d.: not determined.

**Table 2**M<sub>1</sub> receptor agonism, D<sub>2</sub> receptor affinity, hCL<sub>int</sub> and hERG inhibition data for compounds **1–3**, and **5–14**, and reference compounds

Compounds	R <sup>1</sup>	R <sup>2</sup>	hM <sub>1</sub> <sup>a</sup>					
			EC <sub>50</sub> nM	E <sub>max</sub> (%)	hD <sub>2</sub> K <sub>i</sub> (nM) <sup>b</sup>	hCL <sub>int</sub> (L/min)	hERG IC <sub>50</sub> (μM)	ΔMOE logP <sup>c</sup>
<b>1</b>			400	78	5.5	1.4	2.1	—
<b>2</b>		Indol-5-yl	160	70	42	9	4.4	—
<b>3</b>			110	53	9.5	3.9	7.3	—
<b>5</b>			12	69	2200	2.8	>50	−1.3
<b>6</b>			n.d.	0% <sup>d</sup>	1100	9.4	>50	−1.2
<b>7</b>			n.d.	7% <sup>d</sup>	55%	3.6	>50	−1.2
<b>8</b>			20	78	600	1.3	6.3	−0.8
<b>9</b>			73	58	16	5.1	6.6	−0.4
<b>10</b>			n.d.	31%	55	2.3	9.3	−0.3
<b>11</b>			1700	30	1250	3.5	13	−1.2
<b>12</b>			1200	40	>9500	0.9	>50	−1.6

Table 2 (continued)

Compounds	R <sup>1</sup>	R <sup>2</sup>	hM <sub>1</sub> <sup>a</sup>					
			EC <sub>50</sub> nM	E <sub>max</sub> (%)	hD <sub>2</sub> K <sub>i</sub> (nM) <sup>b</sup>	hCl <sub>int</sub> (L/min)	hERG IC <sub>50</sub> (μM)	ΔMOE log P <sup>c</sup>
<b>13</b>			n.d.	4%	1350	1.7	46	−1.6
<b>14</b>			n.d.	8%	650	2.6	22	−1.2
Lu AE51090 ( <b>4</b> )	—	—	61	83	>5000	3.4	20	—
Haloperidol	—	—	n.d.	n.d.	3.0	0.8	1.1	—
ACh	—	—	1.1	100	n.d.	n.d.	n.d.	—

<sup>a</sup> Data are means of two experiments. When an EC<sub>50</sub> could not be established, activity is given as the percent activity at a compound test concentration of 10 μM, as indicated. n.d.: not determined.

<sup>b</sup> Data are means of two experiments. Affinities are expressed as K<sub>i</sub> values (nM) or as percent displacement of radioligands at a compound test concentration of 10 μM, as indicated.

<sup>c</sup> Δ MOElogP values are calculated relative to the corresponding MOElogP value for **3**.

<sup>d</sup> n = 1.

Table 3

M<sub>1</sub> receptor agonism, D<sub>2</sub> receptor affinity, hCl<sub>int</sub> and hERG data for compounds **15–22**

Compounds	R <sup>1</sup>	R <sup>2</sup>	X	hM <sub>1</sub> <sup>a</sup>				
				EC <sub>50</sub> nM	E <sub>max</sub> (%)	hD <sub>2</sub> K <sub>i</sub> (nM) <sup>b</sup>	hCl <sub>int</sub> (L/min)	hERG IC <sub>50</sub> (μM)
<b>15</b>	5-F	H	CH <sub>2</sub>	68	72	60	4.2	5.3
<b>16</b>	6-F	H	CH <sub>2</sub>	n.d.	24%	6.5	6.2	3.4
<b>17</b>	7-F	H	CH <sub>2</sub>	n.d.	23%	90	7.8	5.7
<b>18</b>	8-F	H	CH <sub>2</sub>	300	59	95	5.5	7.9
<b>19</b>	H	4-F	O	n.d.	22%	41	12	6.3
<b>20</b>	H	5-F	O	44	67	14	8.7	4.4
<b>21</b>	H	6-F	O	66	67	2.5	8.8	1.9
<b>22</b>	H	7-F	O	110	51	15	13	3.4

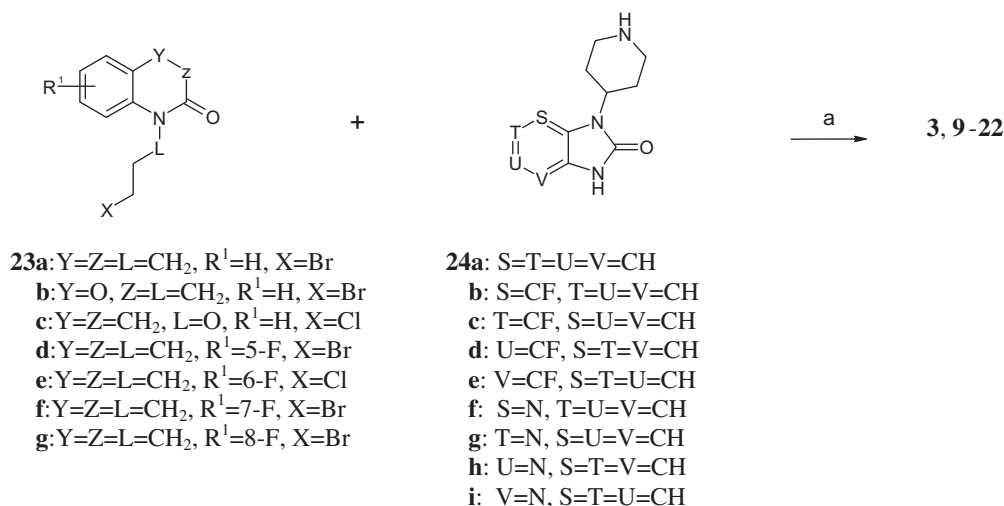
<sup>a</sup> Data are means of two experiments. When an EC<sub>50</sub> could not be established, activity is given as the percent activity at a compound test concentration of 10 μM, as indicated. n.d.: not determined.

<sup>b</sup> Data are means of two experiments. Affinities are expressed as K<sub>i</sub> values (nM) or as percent displacement of radioligands at a compound test concentration of 10 μM, as indicated.

brane domain 6 is mutated to alanine.<sup>20</sup> The Y381 residue is critical for orthosteric binding to the M<sub>1</sub> receptor, and mutation to alanine has been shown to decrease ACh binding affinity 30-fold and drastically reduce its potency about 3,000-fold without affecting the efficacy,<sup>13</sup> making the hM<sub>1</sub> Y381A receptor mutant a useful tool to detect allosteric agonists. Compound **3** was a potent agonist at the hM<sub>1</sub> Y381A receptor mutant, while ACh showed greatly reduced potency (>20,000-fold reduction), suggesting that **3** is activating the hM<sub>1</sub> receptor through interaction with different amino acid residues than ACh, that is an allosteric binding site. The data are summarized in Table 1.

We decided to initiate a hit-to-lead investigation with the aim of concluding whether **3** would be a workable hit, with particular focus on metabolic stability and safety profile. Our strategy was to investigate whether convergent structure–activity relationships (SARs) would allow us to modulate the D<sub>2</sub>/M<sub>1</sub> receptor ratio,

abolish hERG channel inhibition, and obtain acceptable clearance within a compound series based on **3**. Hence, in a small synthetic program, we decided to independently monitor the SAR for D<sub>2</sub> receptor affinity, M<sub>1</sub> receptor agonism, hCl<sub>int</sub> and hERG inhibition. A body of examples exist in the literature of successful medicinal chemistry programs aimed at overcoming hERG channel inhibition. The strategy behind these approaches have been summarized as (a) lowering of log P; (b) reducing basicity; (c) small structural changes; or (d) formation of zwitterions.<sup>21,22</sup> Also, in more general terms, control of log P has been shown to be of great importance in order to manage the pharmacokinetic properties as well as lowering the general risks of toxicity.<sup>23–25</sup> The log P and pK<sub>a</sub> values for **1–4** are given in Chart 1. The pK<sub>a</sub> values of compounds **1**, **3** and **4** were 7.4, 7.6 and 7.9, respectively, which is weakly basic, and furthermore appeared to be uncorrelated to the measured hERG channel inhibition of the individual compounds. We therefore decided to

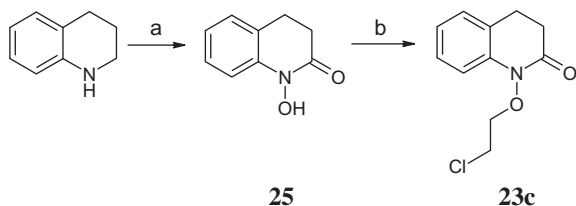


**Scheme 1.** Reagents and conditions: (a) DIPEA, toluene/DMF (1:5), 80 °C.

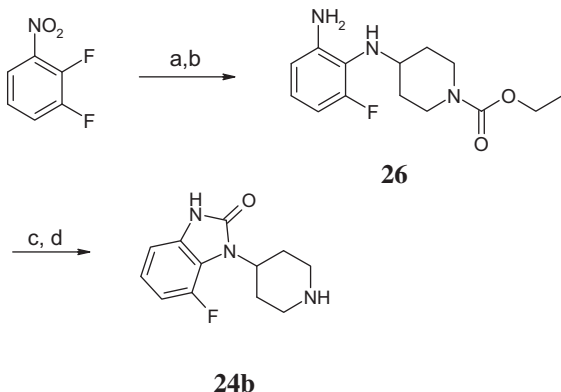
base our hit-to-lead investigation of **3** on lowering log*P*. This can generally be obtained in two ways: (1) through introduction of polarity in the compounds, such as by introduction of heteroatoms, or (2) by removal of lipophilic groups. We opted for the first strategy, and performed a heteroatom scan of compound **3** by synthesis of compounds **5–14**. The results are summarized in Table 2. The experimental log*P* of compound **3** was 2.8, while the calculated log*P* for **3** was 3.3 and 2.7 using the clog*P*<sup>26</sup> or MOE log*P*<sup>27</sup> algorithms, respectively. Based on this, the MOE log*P* algorithm was selected as the best method to estimate the log*P* values of compounds **5–14**. Generally, MOE log*P* calculations suggested Δlog*P* values to be in the order of 1–1.5 log units for CH to N transformations, and to be dependent on the regio-isomeric transformation (Table 2). For CH<sub>2</sub> to O transformations, the calculated changes in MOE log*P* relative to **3** were significantly smaller, and below 0.5 log unit (Table 2). Aza-scanning the aromatic positions of the dihydroquinolinone ring of **3** gave compounds with significantly reduced D<sub>2</sub> receptor affinity (**5–8**) when compared to **3**. In contrast, the effect on M<sub>1</sub> receptor potency was highly dependent on the specific position of the nitrogen atom, with the 5- and 8-aza analogues **5** and **8** showing improved M<sub>1</sub> receptor potency relative to **3**, as well as increased efficacy. In contrast, the 6- and 7-aza isomers **6** and **7** were inactive at the M<sub>1</sub> receptor. The hCl<sub>int</sub> was affected specifically by the position of the introduced nitrogen. Thus, for the 6-aza isomer **6**, the hCl<sub>int</sub> was significantly worsened, while an improvement in clearance was obtained with the 8-aza isomer **8**. The introduction of nitrogen in this region of the molecules generally abolished inhibition of the hERG channel, except for the 8-aza isomer **8**, in which the degree of hERG inhibition was unaltered compared to **3**. Exchange of the dihydroquinolinone moiety of **3** for the oxygen containing benzoxazinone (**9**), had little effect on either the D<sub>2</sub> or M<sub>1</sub> receptor profile, hCl<sub>int</sub> or hERG inhibition. We also prepared the hydroxamic ester derivative **10** in order to polarize the propyl linker region of **3**. Interestingly, this permutation completely removed the M<sub>1</sub> receptor potency and lowered the D<sub>2</sub> receptor affinity, while hCl<sub>int</sub> and hERG channel inhibition remained unchanged relative to **3**. With **9** as a starting point, we next performed an aza-scan of the aromatic positions of the benzimidazolone moiety, leading to compounds **11–14**. A nitrogen atom in any position in this part of the molecule drastically lowered the activity at the primary targets, and also removed the hERG channel inhibition, particularly for the 5-, 6-, and 7-aza isomers **12–14**. The effect on hCl<sub>int</sub> followed the same pattern, with **12** and **13** displaying acceptable intrinsic clearances.

With compounds **3** and **9** as starting points, we decided to fluoro-scan the aromatic positions to identify any potential metabolic hot-spots, as a complement to the SAR investigation based on lowering log*P*. The results are summarized in Table 3. None of the compounds **15–18** and **19–22** showed any improvement of hCl<sub>int</sub> compared to **3** or **9**, respectively. Introduction of fluorine into the aromatic positions of **3** or **9** led to differential effects at the M<sub>1</sub> or D<sub>2</sub> receptors. At M<sub>1</sub> receptors, introduction of fluorine in the 6- or 7-positions of the dihydroquinolinone ring system (**16** and **17**) led to complete loss of potency compared to **3**. This was in contrast to previous results with analogues of **4**.<sup>15</sup> Also, a complete loss of M<sub>1</sub> receptor potency resulted from 4-fluoro substitution at the benzimidazolone ring system (**19**) compared to **9**. Fluorine in other aromatic positions had little or no effect on M<sub>1</sub> receptor potency (**15** and **18** vs. **3**, as well as **20** and **21** vs **9**). Fluorination in the dihydroquinolinone ring system lowered the affinity of the compounds to the D<sub>2</sub> receptor (**15**, **17**, and **18**) compared to **3**, while the 6-fluoro dihydroquinolinone analogue **16** was equipotent to **3**. Fluorination of the benzimidazolone moiety led to differential effects at the D<sub>2</sub> receptors, where a slightly lower affinity compared to **9** resulted from 4-fluorination (**14**), while 6-fluorination increased the potency compared to **9** (compound **21**). In contrast, fluorination in the 5- or 7-positions had no effect on the D<sub>2</sub> receptor affinity (**20** and **22**).

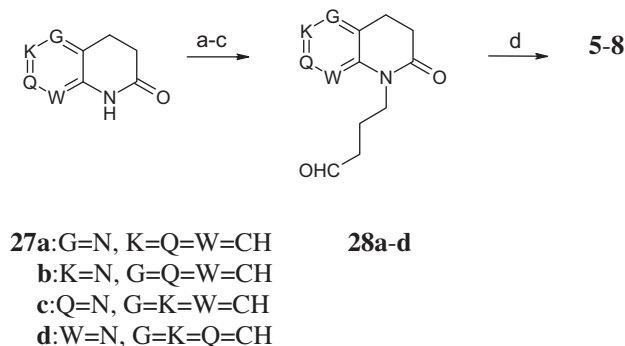
A clear SAR was evident for all four monitored parameters in the present series of compounds. A general and considerable lowering of the inhibition of the hERG channel resulted from lowering log*P* by introduction of nitrogen atoms in the aromatic positions of **3**, with the exception of 8-aza dihydroquinolinone derivative **8**. Introduction of oxygen (**9** and **10**) was calculated to lower the log*P* to a less extent than the aza analogues, and inhibition of the hERG channel was largely unaffected by these permutations when compared to **3**. In contrast, improvement of intrinsic clearance was not achieved by a general lowering of log*P*, but rather seemed to depend on introduction of heteroatoms into specific positions, as exemplified by the 8-aza dihydroquinolinone derivative **8**, or the 5- or 6-aza benzimidazolone derivatives **12** and **13**, respectively. However, a fluoro-scan of the aromatic positions of **3** did not suggest any particular metabolic hot-spots, including the corresponding direct fluorinated analogues of the compounds with improved intrinsic clearance in the aza-scan (**18** vs **8**, **20** vs **12**, and **21** vs **13**). The potency at the M<sub>1</sub> receptor was also influenced by heteroatoms in specific positions, and could be either increased, lowered or completely abolished; and the same was true for substituting



**Scheme 2.** Reagents and conditions: (a)  $\text{Na}_2\text{WO}_4 \cdot 2 \text{H}_2\text{O}$ , 30%  $\text{H}_2\text{O}_2$ , MeOH, 0–20 °C (37% yield); (b) NaH,  $\text{Br}(\text{CH}_2)_2\text{Cl}$ , THF, 0–20 °C (29% yield).



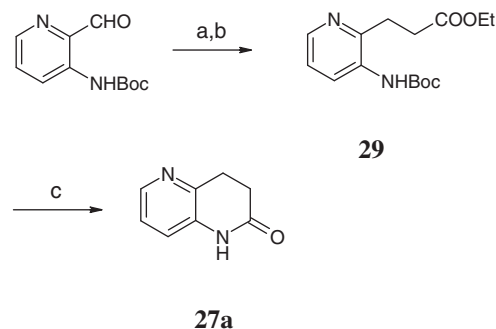
**Scheme 3.** Reagents and conditions: (a)  $\text{Na}_2\text{CO}_3$ , KI, 4-amino-piperidine-1-carboxylic acid ethyl ester, DMF, 50 °C; (b) 5% Pd/C,  $\text{H}_2$ , MeOH, 20 °C; (c) CDI, MeCN, 40 °C; (d) NaOH, EtOH, reflux. (42% overall yield).



**Scheme 4.** Reagents and conditions: (a) NaH, DMSO, 60 °C, then  $\text{Cl}(\text{CH}_2)_3\text{OAc}$ , 20 °C; (b) MeOH,  $\text{KO}^t\text{Bu}$ , 20 °C; (c) IBX, THF, reflux; (d) **24a**,  $\text{NaBH}(\text{OAc})_3$ , THF, AcOH, 20 °C.

fluorine into specific positions of **3**, yet in an uncorrelated manner. In contrast, the  $\text{D}_2$  receptor affinity was generally lowered by lowering of the  $\log P$ , but could be improved by a fluorine at the benzimidazolone 6-position (**21**).

Compounds **3** and **9–22** were prepared by a simple parallel synthesis protocol as described in Scheme 1, by alkylation of piperidyl benzimidazolones **24a–e**, or piperidyl pyridoimidazolones **24f–i** with intermediates **23a–g** in the presence of di-isopropylethyl amine (DIPEA), in a mixed solvent of DMF/toluene (1:5) at 80 °C. The intermediates **23a,b,d–f** were prepared as described in ref. 15, while **23c** was prepared outlined in Scheme 2. Tetrahydroquinoline was treated with sodium wolframate and hydrogenperoxide to yield *N*-hydroxy dihydroquinolinone **25** in 37% yield, which was alkylated with 1-bromo-3-chloropropane in a subsequent step to give **23c** in 29% yield. Compound **24a** was commercially available,



**Scheme 5.** Reagents and conditions: (a) NaH,  $(\text{EtO})_2\text{P}(\text{O})\text{CH}_2\text{CO}_2\text{Et}$ , THF, 25 °C (73% yield); (b) 5% Pd/C,  $\text{H}_2$ , EtOH, 25 °C (67% yield); (c) TFA, DCM, 20 °C (74% yield).

while **24c–e**<sup>28</sup> and **24f–i**<sup>29</sup> were prepared as described in the cited references. The 3-fluoro benzimidazolone **24b** was prepared similarly, as outlined in Scheme 3. Reaction of 1,2-difluoro-3-nitrobenzene with 4-amino piperidine-1-ethylcarbamate, followed by catalytic hydrogenation, afforded intermediate **26**, and **24b** was obtained in 42% overall yield after carbonylation and ring closure using carbonyl diimidazole, followed by deprotection under basic conditions. Compounds **5–8** were synthesized as detailed in Scheme 4. The intermediates **28a–d** were obtained from **27a–d** by alkylation with 3-chloropropylacetate and subsequent saponification, followed by oxidation of the intermediary alcohol with 2-iodoxybenzoic acid (IBX). Reductive amination with **24a** yielded the final products. The intermediates **27b–d** were commercially available, while the preparation of **27a** is described in Scheme 5. Sequential Horner-Wadsworth-Emmons reaction between 2-formyl-pyridin-3-yl-*tert*-butyl carbamate and (diethoxy-phosphoryl)-acetic acid ethyl ester, and catalytic hydrogenation afforded **29** in 49% overall yield, which spontaneously cyclized upon deprotection with TFA to yield **27a** (74% yield).

In conclusion, we designed compound **3**, which had the desired combined  $\text{D}_2$  and  $\text{M}_1$  receptor profile. However, the compound had a high clearance and inhibited the hERG channel. Based on a strategy of lowering  $\log P$ , a hit-to-lead effort was undertaken to clarify whether compounds with combined  $\text{D}_2$  and  $\text{M}_1$  receptor activity and good pharmacokinetic and safety properties could be identified. Although a SAR was evident for all four parameters in question, it was not convergent towards the aim of the investigation. It was possible within this series of compounds to modulate the ratio of activity at the  $\text{D}_2$  and  $\text{M}_1$  receptors, and it was feasible to obtain compounds with  $\text{M}_1$  receptor agonism, acceptable clearance, and weak hERG inhibition. However, a separation between hERG channel inhibition and  $\text{D}_2$  receptor affinity was not possible by this effort. Based on these results, we decided to stop any further investigations of the series based on **3**, and the project was prompted to pursue other avenues.

## Acknowledgement

The authors wish to thank Dr. Klaus Gundertofte for computational assistance.

## Supplementary data

Supplementary data associated with this article can be found, in the online version, at <http://dx.doi.org/10.1016/j.bmcl.2012.05.048>.

## References and notes

- Elvevåg, B.; Goldberg, T. E. *Crit. Rev. Neurobiol.* **2000**, *14*, 1.

2. Elliot, R.; McKenna, P. J.; Robbins, T. J.; Sahakian, B. I. *Cogn. Neuropsych.* **1998**, *3*, 45.
3. Arnt, J.; Bang-Andersen, B.; Dias, R.; Bøgesø, K. P. *Drugs Future* **2008**, *33*, 777.
4. Fischer, A. *Neurotherapeutics* **2008**, *5*, 433.
5. Langmead, C. J.; Watson, J.; Reavill, R. *Pharmacol. Ther.* **2008**, *117*, 232.
6. Sellin, A. K.; Shad, M.; Tammimga, C. *CNS Spect.* **2008**, *13*, 985.
7. Sur, C.; Kinney, G. G. *Curr. Neuropharmacol.* **2005**, *3*, 63.
8. Dean, B.; McLeod, M.; Keriakous, D.; McKenzie, J.; Scarr, E. *Mol. Psychiatry* **2002**, *7*, 1083.
9. Mancama, D.; Arrantz, M. J.; Landau, S.; Kerwin, R. *Am J. Med. Gene. B. Neuropsych. Gene.* **2003**, *119*, 2.
10. Anagnostaras, S. G.; Murphit, G. G.; Hamilton, S. E.; Mitchell, S. L.; Rahnama, N. P.; Nathanson, N. M.; Silva, A. J. *Nat. Neurosci.* **2003**, *6*, 51.
11. Wess, J. *Annu. Rev. Pharmacol. Toxicol.* **2004**, *44*, 423.
12. Lameh, J.; Burstein, E. S.; Taylor, E.; Weiner, D. M.; Vanover, K. E.; Bonhaus, D. W. *Pharmacol. Ther.* **2007**, *115*, 223.
13. Sur, C.; Mallorga, P. J.; Wittmann, M.; Jacobson, M. A.; Pascarella, D.; Williams, J. B.; Brandish, P. E.; Pettibone, D. J.; Scolnick, E. M.; Conn, P. J. *Proc. Natl. Acad. Sci. U.S.A.* **2003**, *100*, 13674.
14. *Human D<sub>2</sub>-receptor binding assay*: The assay was performed as a SPA-based competition-binding assay in a 50 mM Tris pH 7.4 assay buffer containing 120 mM NaCl, 5 mM KCl, 4 mM MgCl<sub>2</sub>, 1.5 mM CaCl<sub>2</sub>, 1 mM EDTA, 1.5 nM [<sup>3</sup>H]-raclopride (Perkin Elmer, NET 975) was mixed with test compound before addition of 20 µg of membranes purified from CHO cells stably transfected with the human D<sub>2L</sub> receptor and 0.25 mg SPA beads (WGA RPNQ 0001, Amersham) in a total volume of 80 µL. The assay plates were incubated for 60 min at room temperature with agitation, and subsequently counted in a scintillation counter (TriLux, Wallac). The total binding, which comprised app 15% of added radioligand, was defined using assay buffer whereas the non-specific binding was defined in the presence of 10 µM haloperidol. The non-specific binding constituted app 10% of the total binding. Data points are expressed in percent of the specific binding of [<sup>3</sup>H]-raclopride and the IC<sub>50</sub> values are determined by non-linear regression analysis using a sigmoidal variable slope curve fitting. The dissociation constant (*K<sub>i</sub>*) were calculated from the Cheng-Prusoff equation (*K<sub>i</sub>* = IC<sub>50</sub>/(1+(L/*K<sub>D</sub>*))), where the concentration of free radioligand L is approximated to the concentration of added [<sup>3</sup>H]-raclopride in the assay. The *K<sub>D</sub>* of [<sup>3</sup>H]-raclopride was determined to 1.5 nM from two independent saturation assays each performed with triplicate determinations.
15. Sams, A. G.; Hentzer, M.; Mikkelsen, G. K.; Larsen, K.; Bundgaard, C.; Plath, C.; Christoffersen, C. T.; Bang-Andersen, B. *J. Med. Chem.* **2010**, *53*, 6386.
16. Inhibition of hERG channel Rb<sup>+</sup> flux: CHO cells stably expressing the hERG channels were plated out in 96 well plates 2 days before the experiment with a cell density of 250,000 cells/ml and 100 µL volume per well. At the day of testing, the media was removed and the cells were added 100 µL RbCl buffer (5.4 mM RbCl, 137 mM NaCl, 8.1 mM Na<sub>2</sub>HPO<sub>4</sub>·2H<sub>2</sub>O, 1.5 mM KH<sub>2</sub>PO<sub>4</sub>, 0.49 MgCl<sub>2</sub>·6 H<sub>2</sub>O, 0.90 mM CaCl<sub>2</sub>, pH 7.2–7.5), and placed in an IGO-Jouan cell incubator at 37 °C and 5% CO<sub>2</sub> for 2–3 h. The cells were washed once in 350 µL Atomic Absorption Spectrometry (AAS) buffer (5.4 mM KCl, 137 mM NaCl, 8.1 mM Na<sub>2</sub>HPO<sub>4</sub>·2H<sub>2</sub>O, 1.5 mM KH<sub>2</sub>PO<sub>4</sub>, 0.49 mM MgCl<sub>2</sub>·6H<sub>2</sub>O, 0.90 CaCl<sub>2</sub>·2H<sub>2</sub>O, pH 7.2–7.5), and the AAS-buffer was removed. To each well was added 120 µL of a solution of test compounds, prepared from DMSO stock solutions (2 or 10 mM) diluted in the high KCl buffer (80.6 mM NaCl, 61.8 mM KCl) to final concentrations in the range: 0.082, 0.205, 0.512, 1.28, 3.2, 8, 20, 50 µM. After incubation for 30 min at room temperature, 100 µL of the supernatant was collected from each well. The cells were washed once in AAS buffer, and lysis buffer (AAS buffer + 1% Triton X100) was added and allowed to stand for 15 min, whereafter 100 µL of lysate was collected from each well. For each well, concentrations of Rb<sup>+</sup> in the supernatant sample and in the cell lysate sample were determined by Atomic Absorption Spectrometry (Thermo Elemental; Solaar; from Thermo Fisher Scientific), and the inhibition of the Rb<sup>+</sup>-flux was calculated from the ratio between concentrations of Rb<sup>+</sup> in the supernatant and in the lysis buffer. Concentration–response curves were obtained from 8 concentrations of test compounds, and IC<sub>50</sub> values for Rb<sup>+</sup> flux inhibition were calculated using the Hill equation with variable slope (equation: Sigmoidal dose–response (variable slope):  $Y = \text{Bottom} + (\text{Top} - \text{Bottom}) / (1 + 10^{-(\log(\text{IC}_{50} - X) * \text{HillSlope}))}$  where X is the logarithm of the concentration, Y is the response; this equation is identical to the 'four parameter logistic equation'.
17. For a description of DMPK assays and in vivo protocols, see: Sams, A. G.; Mikkelsen, G. K.; Larsen, M.; Langgård, M.; Howells, M. E.; Schrøder, T. J.; Brennum, L. T.; Torup, L.; Jørgensen, E. B.; Kreilgård, M.; Bang-Andersen, B. *J. Med. Chem.* **2011**, *54*, 751.
18. Fischer, A. *CNS Drugs* **1999**, *12*, 197.
19. Heinrich, J. N.; Butera, J. A.; Carrick, T.; Kramer, A.; Kowal, D.; Lock, T.; Marquis, K. L.; Paush, M. H.; Popielek, M.; Sun, S.-C.; Tseng, E.; Uveges, A. J.; Mayer, S. C. *Eur. J. Pharmacol.* **2009**, *605*, 53.
20. Spalding, T. A.; Trotter, C.; Skjærbæk, N.; Messier, T. L.; Currier, E. A.; Burstein, E. S.; Li, D.; Hacksell, U.; Brann, M. R. *Mol. Pharmacol.* **2002**, *61*, 1297.
21. Waring, M. J.; Johnstone, C. *Bioorg. Med. Chem. Lett.* **2007**, *17*, 1759.
22. Jamieson, C.; Moir, E. M.; Rankovic, Z.; Wishart, G. J. *Med. Chem.* **2006**, *49*, 5029.
23. Gleeson, M. P. *J. Med. Chem.* **2008**, *51*, 817.
24. Leeson, P. D.; Springthorpe, B. *Nat. Rev. Drug. Disc.* **2007**, *6*, 881.
25. Hughes, J. D.; Blagg, J.; Price, D. A.; Bailey, S.; DeCrescenzo, G. A.; Devraj, R. V.; Ellsworth, E.; Fobian, Y. M.; Gibbs, M. E.; Gilles, R. W.; Greene, N.; Huang, E.; Krieger-Burke, T.; Loesel, J.; Whiteley, L.; Zhang, Y. *Bioorg. Med. Chem. Lett.* **2008**, *18*, 4872.
26. Daylight, version 4.8.
27. MOE version 2009.10.
28. Gustin, D. J.; Sehon, C. A.; Wei, J.; Cai, H.; Meduna, S. P.; Khatuya, H.; Sun, S.; Gu, Y.; Jiang, W.; Thurmond, R. L.; Karlsson, L.; Edwards, J. P. *Bioorg. Med. Chem. Lett.* **2005**, *15*, 1687.
29. Burgey, C. S.; Stump, C. A.; Williams, T. M. WO 2005/013894 A2.